Nanoscale

PAPER

View Article Online
View Journal

Cite this: DOI: 10.1039/c5nr07329d

A facile and low-cost length sorting of single-wall carbon nanotubes by precipitation and applications for thin-film transistors†

Hui Gui,[a] Haitian Chen,[b] Constantine Y. Khripin,[c] Bilu Liu,[b] Jeffrey A. Fagan,[c] Chongwu Zhou*[b] and Ming Zheng*[c]

Received 21st October 2015,
Accepted 14th December 2015

DOI: 10.1039/c5nr07329d

www.rsc.org/nanoscale

Semiconducting single-wall carbon nanotubes (SWCNTs) with long lengths are highly desirable for many applications such as thin-film transistors and circuits. Previously reported length sorting techniques usually require sophisticated instrumentation and are hard to scale up. In this paper, we report for the first time a general phenomenon of a length-dependent precipitation of surfactant-dispersed carbon nanotubes by polymers, salts, and their combinations. Polyelectrolytes such as polymethacrylate (PMAA) and polystyrene sulfonate (PSS) are found to be especially effective on cholate and deoxycholate dispersed SWCNTs. By adding PMAA to these nanotube dispersions in a stepwise fashion, we have achieved nanotube precipitation in a length-dependent order: first nanotubes with an average length of 650 nm, and then successively of 450 nm, 350 nm, and 250 nm. A similar effect of nanotube length sorting has also been observed for PSS. To demonstrate the utility of the length fractionation, the 650 nm-long nanotube fraction was subjected to an aqueous two-phase separation to obtain semiconducting enriched nanotubes. Thin-film transistors fabricated with the resulting semiconducting SWCNTs showed a carrier mobility up to 18 cm^2 $(V\ s)^{-1}$ and an on/off ratio up to 10^7. Our result sheds new light on the phase behavior of aqueous nanotube dispersions under high concentrations of polymers and salts, and offers a facile, low-cost, and scalable method to produce length sorted semiconducting nanotubes for macroelectronics applications.

Introduction

Single-wall carbon nanotubes (SWCNTs) have unique electrical properties which make them promising candidates for future applications in nanoelectronics and macroelectronics.[1–4] The structural polydispersity of SWCNTs, both in their atomic structures and in their length, is, however, a major issue that needs to be solved to enable their applications in electronics and many other areas. Significant progress in nanotube separation according to metallic/semiconducting character, chirality, and diameter has been made utilizing effective methods such as ion exchange chromatography (IEX),[5,6] density gradient ultracentrifugation (DGU),[7] gel chromatography,[8–10] polymer selective wrapping,[11] and aqueous two-phase (ATP) extraction.[12–19]

Addressing SWCNT length polydispersity to improve application performances is motivated by numerous publications reporting length-dependent results.[20–26] For example, short nanotubes are more effective for drug delivery,[23,24] while long tubes are preferred in SWCNT thin-film transistors (TFTs).[21,25–27] In the nanotube network TFTs, the removal of shorter tubes is important because along a conducting path longer nanotubes would form fewer tube–tube junctions than shorter nanotubes. As a result, networks formed by longer nanotubes are expected to exhibit lower sheet resistance, higher on-current, and higher carrier mobility.[3,26] Because the as-prepared nanotube dispersions usually have broad length distributions, the examples above indicate that in addition to the metal/semiconductor and chirality sorting, it is also highly desirable to sort SWCNTs based on their lengths.

Several methods have been reported for the SWCNT length sorting. Size exclusion chromatography (SEC)[28,29] has been used for nanotube length sorting to achieve narrow length distributions. Other methods such as ultracentrifugation,[30,31] cross flow filtration,[32] and flow-field flow fractionation,[33] have also been employed for the length sorting of nanotubes.

[a]Department of Chemical Engineering and Materials Science, University of Southern California, Los Angeles, CA 90089, USA
[b]Department of Electrical Engineering, University of Southern California, Los Angeles, CA 90089, USA. E-mail: chongwuz@usc.edu
[c]Materials Science and Engineering Division, National Institute of Standards and Technology, Gaithersburg, MD 20899, USA. E-mail: ming.zheng@nist.gov
†Electronic supplementary information (ESI) available. See DOI: 10.1039/c5nr07329d

However, the above-mentioned methods require expensive instrumentation and are not readily scalable. Recently, some of us (C. Y. K. and M. Z.) reported that a polymer precipitation[34] method can be used to effectively sort SWCNTs by their lengths. In this method, a charge-neutral polymer, polyethylene glycol (PEG), is introduced to a dispersion of DNA-wrapped SWCNTs, inducing a molecular-crowding effect that leads to length-dependent nanotube precipitation. In comparison with the other methods mentioned above, this polymer precipitation method does not require expensive instruments, and is a facile and scalable length sorting method. The demonstration of the method was limited however to ss-DNA and RNA dispersed SWCNTs, and was not reported for SWCNTs dispersed *via* any of the much more broadly utilized surfactants.

Given the desirability to fractionate SWCNT dispersions by length, the utility of implementing a similar precipitation method to length sort SWCNT dispersions made with low-cost surfactants is clear. Unfortunately, adding PEG alone to SWCNTs dispersed with the commonly used surfactant sodium deoxycholate (SDC) does not readily result in SWCNT precipitation. We found however that the addition of an extra salt, such as NaSCN, to the mixture of PEG and SDC-SWCNT dispersion, re-enables selective precipitation. This prompted us to conduct a systematic investigation on the general phenomenon of the polymer and salt induced precipitation of the surfactant dispersed carbon nanotubes.

In this paper, we report an important extension of the polymer precipitation method to the length sorting of the surfactant-dispersed SWCNTs. In particular, we show that two polyelectrolytes – polymethacrylate (PMAA) and polystyrene sulfonate (PSS), can be applied to SDC-dispersed SWCNTs to achieve a precipitation based nanotube length fractionation. Significantly, we show that applying this new length-sorting methodology to low-cost raw nanotubes from the plasma torch method results in fractions of relatively long and uniform length SWCNTs suitable for subsequent multistep ATP extraction of the metallic and semiconducting SWCNT subpopulations. TFTs fabricated with the resulting semiconducting SWCNTs exhibit excellent performance with a mobility as high as 18 cm^2 $(V\ s)^{-1}$ and I_{on}/I_{off} ratio up to 10^7.

Materials and methods

Certain commercial equipment, instruments, or materials are identified in this paper in order to specify the experimental procedure adequately. Such identification is not intended to imply recommendation or endorsement by the National Institute of Standards and Technology, nor is it intended to imply that the materials or equipment identified are necessarily the best available for the purpose. Unless noted otherwise, all reagents were obtained from standard sources.

Materials

Raw plasma torch SWCNTs were purchased from Raymor Nanotech (lot number RNL 13-020-016). PMAA (40%, 4–6 kDa), PSS (30%, 70 kDa, 200 kDa, and 1000 kDa), sodium polyacrylate (PAA, 10 kDa), polyvinylpyrrolidone (PVP, 10 kDa), SDC, sodium chlorate (SC), sodium dodecyl sulfate (SDS), NaSCN, NaClO, $(NH_4)_2SO_4$ and Triton X-405 were purchased from Sigma-Aldrich; PEG (6 kDa), and dextran (DX, 70 kDa) were purchased from Alfa Aesar and Tokyo Chemical Industries (TCI) respectively. Poly-L-lysine (0.1% w/v) was purchased from TED Pella, Inc. All chemicals were used as received.

SWCNT dispersion

Plasma torch SWCNTs were dispersed in 20 g L^{-1} SDC at 4 mg mL^{-1} by sonication (tip sonicator, 0.64 cm, Thomas Scientific). The sonication condition was 1 h at about 0.9 W mL^{-1}. The sonication vial was placed in an ice bath to maintain low temperature. After sonication, the suspension was centrifuged for 2 h at 1885 rad s^{-1} (18 krpm) at 10 °C in a JA-20 rotor (Beckman-Coulter). After centrifugation the supernatant was decanted and used as the parent dispersion for the length sorting experiments.

Polyelectrolyte precipitation

Two schemes for sequential precipitation were used in this work following previous reports.[34] In forward sequential precipitation, appropriately diluted PMAA or PSS solution was mixed with the SWCNT dispersion to the final polymer concentration of 1 wt%. The mixture was vortexed and then incubated for 4 h at room temperature (23 °C). A mild 5 min centrifugation at 943 rad s^{-1} (9 krpm, JA-20 rotor, Beckman-Coulter), is then sufficient to pellet a fraction of the SWCNT mass, referred to hereafter as the "precipitate" or "pellet". After removing the supernatant, the pellet was resuspended in 2 wt% SC, and the fraction was labelled as "1% PMAA (or PSS)". Additional PMAA or PSS was then added to the supernatant to increase the polymer concentration (to 2 wt%, 4 wt%, and finally 6 wt%), and the above precipitation steps were repeated to yield additional pellet fractions. In reverse sequential precipitation, the highest polymer concentration is used in the initial step. In this method the supernatant is retained as the sorted fraction, and a lesser polymer concentration solution is added to dilute and resuspend the pellet; the resuspended pellet is then incubated/pelleted to produce the next sequential fraction.

Multistep ATP extraction

We followed the general procedure given by Khripin *et al.*[12] and Gui *et al.*[14] For the plasma torch SWCNTs, 3–5 steps were needed to obtain a top phase that is highly enriched in semiconducting nanotubes. To remove the polymers, we added 0.1 M NaSCN to the top phase and precipitated out all SWCNTs to form a small volume pellet with light centrifugation (5 min, 943 rad s^{-1} (9 krpm)). The pellet was resuspended in 0.4% SC + 0.1% SDS, and was used directly for thin film deposition.

Optical absorption characterization

A Varian Cary 5000 spectrometer was used to characterize the UV-vis-NIR absorption of the nanotubes. For liquid samples

spectra were recorded through a quartz microcuvette with a 10 mm path length.

Thin-film transistor fabrication

To form a SWCNT network on a Si/SiO_2 substrate, we first prepared poly-L-lysine functionalized substrates according to a previously reported procedure.[35] Functionalized substrates were then immersed in the SWCNT solution for 5.5 h. Subsequently the substrate was rinsed with deionized (DI) water and blow dried with N_2. A 50 nm SiO_2 layer was used as the back-gate dielectric. Standard photolithography for TFT fabrication was used as described previously.[36]

Atomic force microscopy (AFM)

Clean Si/SiO_2 substrates were used for the SWCNT deposition. The SC-dispersed SWCNT sample was diluted 5 times with around 0.1 M NaSCN and was deposited onto the substrate by a 5–10 min incubation. After incubation, samples were rinsed with DI water and blow dried using nitrogen. AFM imaging was done on a Bruker Dimension Icon AFM in the peak-force tapping mode (ScanAsyst) using the respective ScanAsyst-Air probes. Typically, more than one hundred SWCNTs from each fraction were measured for statistical analysis.

Results and discussion

Polymer and salt precipitation of surfactant dispersed SWCNTs – a general phenomenon

Polymer precipitation *via* a molecular-crowding-induced cluster formation has been used to fractionate DNA-wrapped nanotubes according to their lengths.[34] In this work, we found that the precipitation of SWCNT dispersions is a general phenomenon: it can be induced by addition of polymers, salts, and their combinations, and is applicable to a variety of aqueous SWCNT dispersions. For SWCNTs dispersed by anionic surfactants (*e.g.* SDC, SC, SDBS, DNA), length-dependent precipitation can be induced by addition of many different chemicals. These include (1) neutral polymers such as PEG, poly(2-ethyl-2-oxazoline), and PVP when in combination with added salt such as NaSCN; (2) anionic polyelectrolytes such as PMAA, PSS and PAA; and (3) salt alone at sufficiently high concentrations. For SWCNTs dispersed by neutral surfactants such as Triton X-405, $(NH_4)_2SO_4$ was identified as a very effective agent to induce length-dependent precipitation.

Our observations strongly suggest that nanotube precipitation cannot be fully accounted for by a simple depletion force based mechanism[34] proposed for charge-neutral crowding agents. Further investigations are needed to understand the physical mechanism behind the general precipitation phenomenon. We suggest that the physics behind the phenomenon is that of phase separation of two substances (SWCNTs, and polymers and/or salt) at sufficiently high concentrations: the precipitated is the SWCNT-rich phase, and the supernatant is the polymer and/or salt-rich phase. Since longer tubes contribute less entropy to the free energy of the SWCNT-rich phase than shorter tubes with the same mass fraction, it is expected that longer tubes undergo phase separation more readily than shorter tubes. This is analogous to the well-studied polymer–polymer phase separation, where longer-chain polymers are more readily phase-separated.[37]

Length sorting by polyelectrolytes

We found that polyelectrolytes, such as PMAA or PSS are the most convenient to use for the precipitation of surfactant-dispersed nanotubes. A schematic of the forward precipitation scheme using these molecules is illustrated in Fig. 1. The structures of PMAA and PSS are shown in Fig. 1b. As the polymer concentration increases gradually, progressively shorter and shorter tubes are precipitated out. Length sorting can thus be achieved by repeated cycles of polymer addition and SWCNT pellet removal (Fig. 1c).

In this work, we used inexpensive raw SWCNTs mass-produced by the plasma torch method. The price of the plasma torch SWCNTs is about 10 times lower than that of arc discharge SWCNTs; however the as-synthesized plasma torch SWCNTs contain a large amount of impurities such as C_{60}, amorphous carbon and catalysts. SDC was used to disperse the raw SWCNTs. A detailed dispersion preparation method is given in the Materials and methods section. To initiate the forward sequential precipitation process, we added PMAA at a final concentration of 1% to the SWCNT dispersion. After thorough mixing and shaking, mild centrifugation was used to collect the precipitated pellet. The supernatant was collected and extra PMAA was added to the final concentration of 2% to precipitate out more SWCNTs. The procedure was then repeated at PMAA concentrations of 4% and 6% respectively, as shown in Fig. 1c. Each precipitated pellet was collected and resuspended in 2% SC. UV-vis-NIR absorption spectra of the re-dispersed pellets are shown in Fig. S1.† The spectra indicate that the precipitation sorting process caused some minor changes in the diameter distribution.

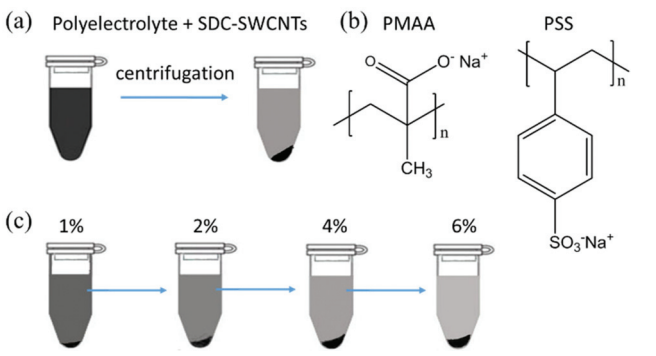

Fig. 1 (a) Schematic showing that adding polyelectrolyte (PMAA or PSS) to SDC-dispersed SWCNTs leads to nanotube precipitation. (b) Molecular structures of PMAA and PSS. (c) Length-sorting by forward sequential polymer addition and SWCNT precipitation.

We then characterized the length distribution of the precipitated fractions using AFM. Fig. 2a–d show the AFM images of SWCNTs collected from 1%, 2%, 4% and 6% PMAA precipitation. It is evident that as the PMAA concentration increases from 1% to 6%, the average length of the sorted SWCNTs decreases gradually. To be more quantitative, we have measured the lengths of more than 100 nanotubes from each of the four precipitated fractions. Fig. 2e shows a length distribution histogram for the 1% and 4% PMAA precipitated fractions. SWCNTs from the 1% PMAA precipitation are distributed mainly in the 0.4 to 0.7 μm length range, while SWCNTs from the 4% PMAA precipitation pellet are more generally in the 0.1 to 0.5 μm length range. Statistical analysis (Fig. 4f) shows that the average tube length is 0.65 μm, 0.45 μm, 0.35 μm, and 0.25 μm for the 1%, 2%, 4% and 6% PMAA precipitated fractions, respectively. These results demonstrate that a simple PMAA precipitation can yield a clear length sorting of the surfactant-dispersed nanotubes: longer nanotubes are precipitated out at lower PMAA concentrations and then shorter and shorter nanotubes are precipitated out as PMAA concentration increases.

Besides PMAA, we have also used another polyelectrolyte PSS to achieve a nanotube length sorting by the forward sequential precipitation method (Fig. 1c). The AFM images in Fig. 3a–d are from 1%, 2%, 4% and 6% PSS fractions. Fig. 3e and f provide length distribution statistics for the PSS precipitated tubes.

Previous studies have shown that the optimal PEG molecular weight range is 6–12 kDa for the length sorting of DNA-wrapped nanotubes.[34] To investigate the polymer chain length effect on length sorting of surfactant dispersed SWCNTs, we tested PSS polymers with molecular weights of 70 kDa, 200 kDa and 1000 kDa, respectively, and found similar length sorting effects (Fig. S2†).

What we have described so far are results from the forward sequential precipitation, *i.e.* increasing the polymer concentration gradually to precipitate out longer tubes first. Alternatively, a reverse sequential precipitation as shown in Fig. 4a can also be used for length sorting. In this case, one starts the precipitation with the highest polymer concentration to obtain shorter tubes in the supernatant first, then gradually reduces the concentration of the added polymer to the re-dispersed

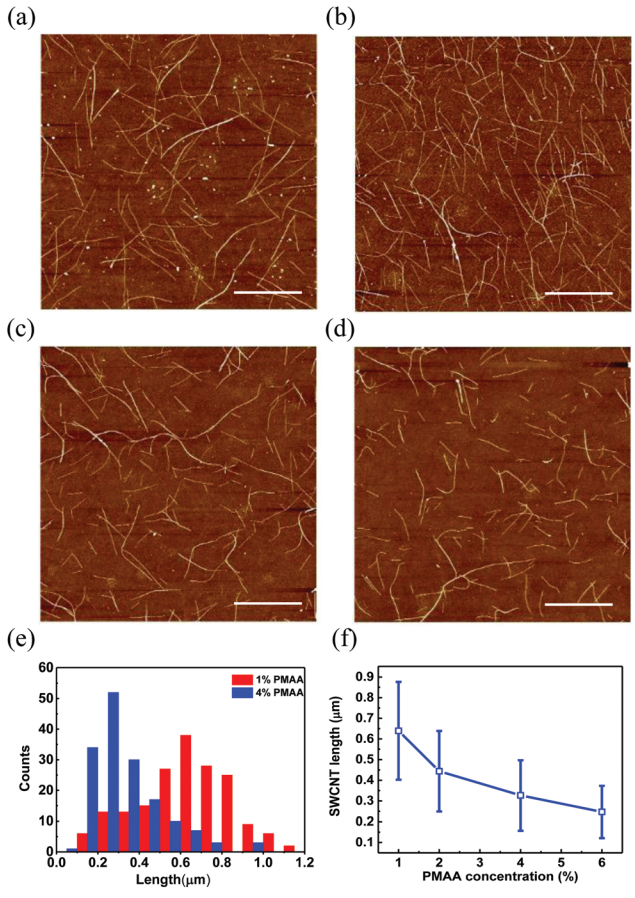

Fig. 2 AFM images of nanotubes from the (a) 1%, (b) 2%, (c) 4%, and (d) 6% PMAA fractions. The scale bar is 1 μm for all images. (e) Length distributions of SWCNTs from the 1% and 4% PMAA fractions. (f) Average tube lengths of the 1%, 2%, 4% and 6% PMAA fractions.

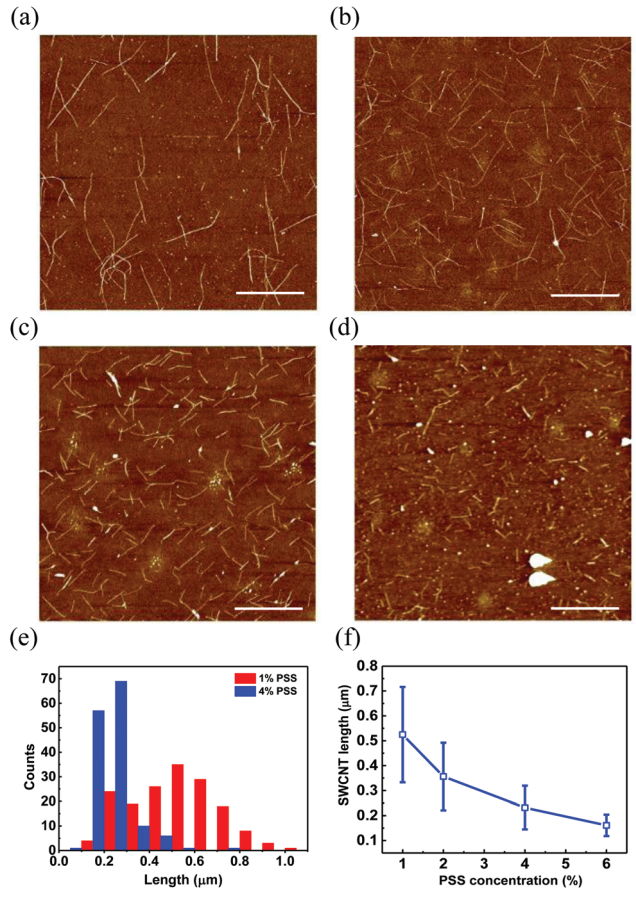

Fig. 3 AFM images of nanotubes from the (a) 1%, (b) 2%, (c) 4%, and (d) 6% PSS fractions. The scale bar is 1 μm for all images. (e) Length distributions of the 1% and 4% PSS fractions. (f) Average tube lengths of the 1%, 2%, 4% and 6% PSS fractions.

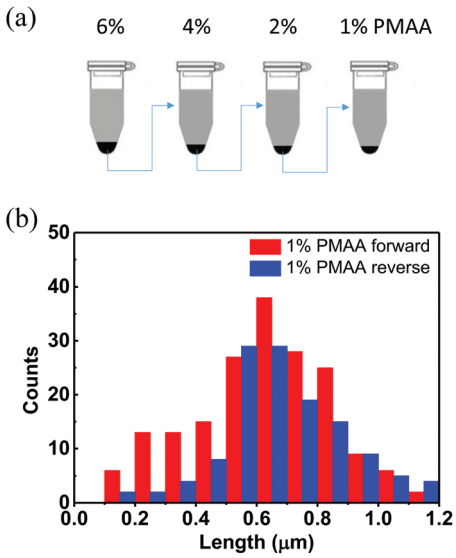

Fig. 4 (a) Schematic of reverse sequential precipitation of SWCNTs, where precipitations using 6%, 4%, 2%, and 1% PMAA were conducted sequentially. (b) Length distributions of SWCNTs obtained by forward and reverse precipitation using 1% PMAA.

pellet to obtain progressively longer tubes. By comparing length distributions of the longest tube fractions obtained by the forward and reverse precipitations, we found that they yield similar length distributions, except that the fraction from the forward precipitation contained in general more short tubes from 0.1 to 0.4 μm. As a result, nanotubes from forward precipitation have an average length of 0.65 μm, slightly shorter than reverse precipitation which has an average length of 0.7 μm. This is understandable, as reverse precipitation removes shorter nanotubes at each precipitation step (4 steps in total) and at last only the longest nanotubes will survive, while forward precipitation only has one step to remove shorter nanotubes from the longest fraction.

ATP separation and thin film transistors

The length sorted nanotubes can be further processed to achieve the enrichment of semiconducting nanotubes for electronic applications. Here we used the ATP extraction method for metallic/semiconducting SWCNT separation. The 1% PMAA precipitated SWCNTs with an average length of 650 nm, were resuspended in 2% SC and directly used for ATP separation. Detailed information on the separation is given in the Materials and methods section. Fig. 5a shows the absorption spectra of the starting SWCNT dispersion (black trace), and semiconducting tube fraction 1-R extracted from the long nanotubes of the 1% PMAA fraction (red trace). The latter spectrum shows no metallic absorption features in the metallic transition region (M11, wavelengths ≈600 nm–800 nm). The short nanotubes of the 6% PMAA fraction have also been separated by ATP to yield a semiconducting SWCNT enriched fraction (6-R), the absorption spectrum of which is shown in Fig. S3.† We found that it is easier to enrich semiconducting nanotubes from longer tube fractions, while more steps are needed to achieve the same semiconducting purity using shorter tube fractions. Polymers in the 1-R and 6-R fractions were removed by introducing 0.1 M NaSCN to precipitate out the nanotubes, and then re-suspending the pelleted nanotubes in a mixture of 0.4% SC + 0.1% SDS for easier deposition on a Si/SiO_2 substrate to form thin-film networks. It is worth noting that in addition to length fractionation, precipitation is also a convenient way to remove non-nanotube chemicals such as excess amount of surfactants, graphitic impurities, and polymers in nanotube fractions obtained from ATP separations (these components are assumed to partition volumetrically and thus are vastly reduced in a precipitation/dilution sequence).

To demonstrate the utility of the length-sorted semiconducting nanotubes, we fabricated TFTs using the longest semiconducting fraction 1-R, since long nanotubes are expected to have few nanotube–nanotube junctions along a conducting path, and therefore a higher on-current and mobility. The SEM image of a typical thin-film network made of the 1-R fraction is shown in Fig. 5b. Using the thin-film network made of the 1-R tubes, we fabricated back-gated transistors. The channel widths (W) of the devices were chosen to be (200, 400, 800, 1200, 1600, and 2000) μm, while channel lengths (L) were (4, 10, 20, 50 and 100) μm. Fig. 5c shows a typical forward and reverse drain current-*versus*-gate voltage (I_D–V_G) of a device with L = 4 μm and W = 400 μm, indicating p-type transfer characteristics. The output characteristics, *i.e.* drain current *versus* drain voltage (I_D–V_D) plotted at different gate voltages in both the linear regime (−0.1 V–0.1 V) and the saturation regime (−3 V–0 V) are shown in Fig. S4.† In the linear regime at small V_D, the contacts formed between metal electrodes and the nanotubes are Ohmic contacts. When V_D is more negative, drain current saturation is observed, indicating a well-behaved field-effect operation. Fig. 5d is the on-current density *versus* channel length (I_D/W–L). The on-current density is inversely proportional to the channel length, demonstrating high uniformity of the devices. The highest on-current density is 0.75 μA μm^{-1}, which is comparable to the literature reports.[38,39]

Fig. 5e shows the I_{on}/I_{off} ratio *versus* channel length for TFTs made with the 1-R nanotubes. We can see that the on/off ratio is higher than 10^5 even at the shortest channel length (4 μm). When the channel length is increased to 20 μm, the on/off ratio is improved to 10^7. There is a slight decrease of the on/off ratio to 10^6 when the channel length is further increased to 50 μm and 100 μm. This is because the off-current decreases due to the lower probability of forming a percolation path at longer channel lengths, and when it becomes comparable to the noise level of the measurement equipment[36] there will be a slight decrease of the on/off ratio. Except for those that have channel lengths of 4 μm, all the TFT devices have an on/off ratio higher than 10^6. The on/off ratio of the TFTs we fabricated is comparable to the highest values reported in the literature.[40] Fig. 5f is a plot of the mobility

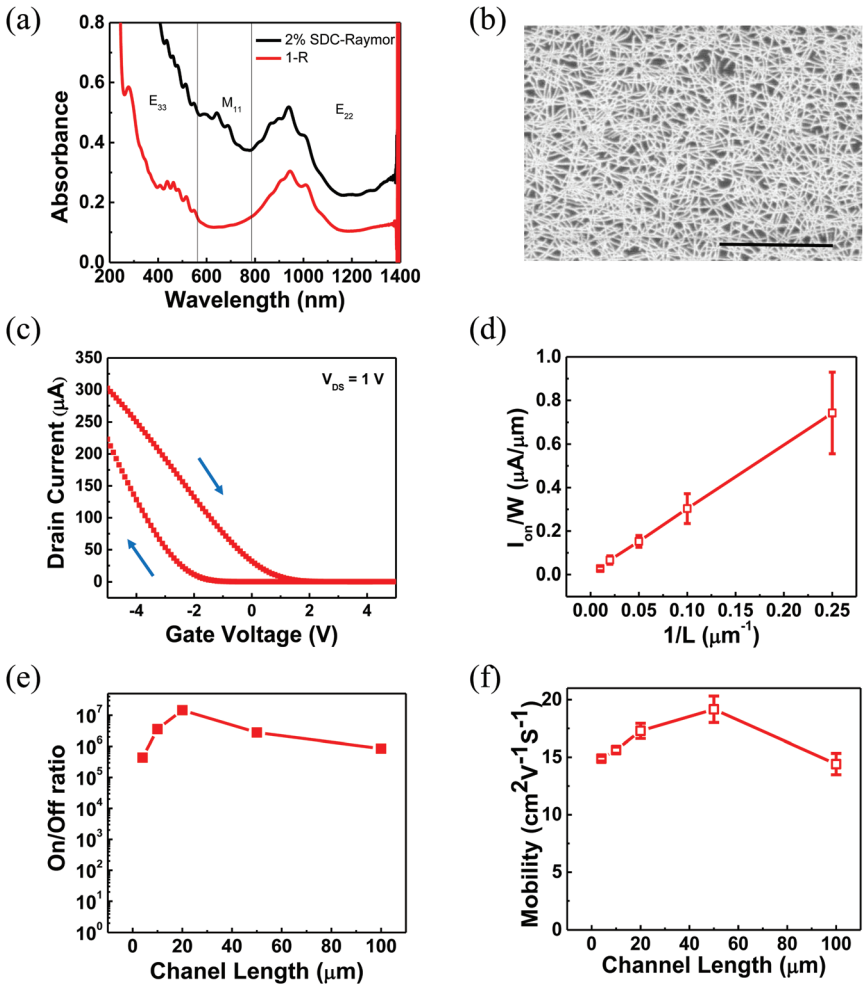

Fig. 5 (a) Absorption spectra of unsorted (black trace) plasma torch SWCNTs and the semiconducting SWCNT enriched 1-R fraction (red trace). (b) An SEM image of the 1-R nanotube thin-film network on a Si/SiO_2 substrate. The scale bar is 2 μm. (c) Transfer characteristics of TFTs fabricated with the 1-R fraction with L = 4 μm and W = 400 μm. The blue arrows indicate the forward and reverse scanning directions. (d) On-current density *versus* inverted channel length of TFTs fabricated with the 1-R fraction. (e) On/off ratio *versus* channel length of TFTs. (f) Relationship of mobility and channel length of TFTs made with the 1-R fraction.

versus channel length for the devices. The mobility, which is calculated based on the parallel plate model, ranges from 14 to 18 cm^2 $(V\ s)^{-1}$, indicating good uniformity in device performance. At 20 μm channel length, the on/off ratio is the highest and reaches 10^7 while the mobility remains at 17 cm^2 $(V\ s)^{-1}$. At 50 μm channel length, the mobility reaches the maximum of 18 cm^2 $(V\ s)^{-1}$ and the on/off ratio remains higher than 10^6. The mobility we obtain is higher than other random nanotube network TFTs.[36] We also fabricated TFTs using the shortest fraction 6-R. While the on/off ratio of TFTs made with 6-R is similar to those made with 1-R, the on-current density (maximum 0.26 μA μm^{-1}) and mobility (1–4 cm^2 $(V\ s)^{-1}$) are much lower (Fig. S5 in the ESI†). These data demonstrate that high performance TFT devices with high on-current density, on/off ratio and mobility can be fabricated using the inexpensive raw plasma torch SWCNTs after length sorting and metal/semiconductor separation.

Conclusions

In this work, we have expanded the precipitation based length sorting method to surfactant-dispersed SWCNTs. Utilizing the polyelectrolytes PMAA and PSS, we realized the separation of surfactant-dispersed nanotubes by their lengths. The length-sorted SWCNT fractions were found to be readily further separable by ATP for the semiconducting tube enrichment. We applied the facile length sorting and M/S separation methods to the low-cost plasma torch SWCNTs. TFTs fabricated with long semiconducting nanotubes showed on/off ratios of 10^5–10^7 and mobilities of 14–18 cm^2 $(V\ s)^{-1}$. Our findings shed new light on the phase behaviour of colloidal SWCNTs at high polymer and salt concentrations, and demonstrate that precipitation-based length sorting has great potential as a facile, low-cost and scalable method to produce length sorted semiconducting nanotubes for macroelectronics applications.

Acknowledgements

We acknowledge financial support from AFOSR and Joint King Abdulaziz City for Science and Technology (KACST)/California Center of Excellence.

References

1 M. M. Shulaker, G. Hills, N. Patil, H. Wei, H.-Y. Chen, H. S. P. Wong and S. Mitra, *Nature*, 2013, **501**, 526–530.
2 C. Wang, J. Zhang and C. Zhou, *ACS Nano*, 2010, **4**, 7123–7132.
3 S. J. Kang, C. Kocabas, T. Ozel, M. Shim, N. Pimparkar, M. A. Alam, S. V. Rotkin and J. A. Rogers, *Nat. Nanotechnol.*, 2007, **2**, 230–236.
4 A. D. Franklin, *Science*, 2015, **349**, aab2750.
5 X. Tu, S. Manohar, A. Jagota and M. Zheng, *Nature*, 2009, **460**, 250–253.
6 M. Zheng and E. D. Semke, *J. Am. Chem. Soc.*, 2007, **129**, 6084–6085.
7 M. S. Arnold, A. A. Green, J. F. Hulvat, S. I. Stupp and M. C. Hersam, *Nat. Nanotechnol.*, 2006, **1**, 60–65.
8 K. Moshammer, F. Hennrich and M. M. Kappes, *Nano Res.*, 2009, **2**, 599–606.
9 H. Liu, D. Nishide, T. Tanaka and H. Kataura, *Nat. Commun.*, 2011, **2**, 309.
10 H. Gui, H. Li, F. Tan, H. Jin, J. Zhang and Q. Li, *Carbon*, 2012, **50**, 332–335.
11 A. Nish, J. Y. Hwang, J. Doig and R. J. Nicholas, *Nat. Nanotechnol.*, 2007, **2**, 640–646.
12 C. Y. Khripin, J. A. Fagan and M. Zheng, *J. Am. Chem. Soc.*, 2013, **135**, 6822–6825.
13 J. A. Fagan, C. Y. Khripin, C. A. Silvera Batista, J. R. Simpson, E. H. Haroz, A. R. Hight Walker and M. Zheng, *Adv. Mater.*, 2014, **26**, 2800–2804.
14 H. Gui, J. K. Streit, J. A. Fagan, A. R. Hight Walker, C. Zhou and M. Zheng, *Nano Lett.*, 2015, **15**, 1642–1646.
15 J. A. Fagan, E. H. Haroz, R. Ihly, H. Gui, J. L. Blackburn, J. R. Simpson, S. Lam, A. R. Hight Walker, S. K. Doorn and M. Zheng, *ACS Nano*, 2015, **9**, 5377–5390.
16 G. Ao, C. Y. Khripin and M. Zheng, *J. Am. Chem. Soc.*, 2014, **136**, 10383–10392.
17 N. K. Subbaiyan, S. Cambré, A. N. G. Parra-Vasquez, E. H. Hároz, S. K. Doorn and J. G. Duque, *ACS Nano*, 2014, **8**, 1619–1628.
18 N. K. Subbaiyan, A. N. G. Parra-Vasquez, S. Cambré, M. A. S. Cordoba, S. E. Yalcin, C. E. Hamilton, N. H. Mack, J. L. Blackburn, S. K. Doorn and J. G. Duque, *Nano Res.*, 2015, **8**, 1755–1769.
19 L. Wei, B. Liu, X. Wang, H. Gui, Y. Yuan, S. Zhai, A. K. Ng, C. Zhou and Y. Chen, *Adv. Electron. Mater.*, 2015, **1**.
20 Z. L. Wang, D. W. Tang, X. B. Li, X. H. Zheng, W. G. Zhang, L. X. Zheng, Y. T. Zhu, A. Z. Jin, H. F. Yang and C. Z. Gu, *Appl. Phys. Lett.*, 2007, **91**, 123119.
21 D. Simien, J. A. Fagan, W. Luo, J. F. Douglas, K. Migler and J. Obrzut, *ACS Nano*, 2008, **2**, 1879–1884.
22 B. Liu, W. Ren, C. Liu, C. H. Sun, L. Gao, S. Li, C. Jiang and H. M. Cheng, *ACS Nano*, 2009, **3**, 3421–3430.
23 R. P. Feazell, N. Nakayama-Ratchford, H. Dai and S. J. Lippard, *J. Am. Chem. Soc.*, 2007, **129**, 8438–8439.
24 M. L. Becker, J. A. Fagan, N. D. Gallant, B. J. Bauer, V. Bajpai, E. K. Hobbie, S. H. Lacerda, K. B. Migler and J. P. Jakupciak, *Adv. Mater.*, 2007, **19**, 939–945.
25 Y. Miyata, K. Shiozawa, Y. Asada, Y. Ohno, R. Kitaura, T. Mizutani and H. Shinohara, *Nano Res.*, 2011, **4**, 963–970.
26 Y. Kuwahara, F. Nihey, S. Ohmori and T. Saito, *Carbon*, 2015, **91**, 370–377.
27 R. Si, H. Wang, L. Wei, Y. Chen, Z. Wang and J. Wei, *J. Mater. Res.*, 2012, **28**, 1004–1011.
28 X. Huang, R. S. McLean and M. Zheng, *Anal. Chem.*, 2005, **77**, 6225–6228.
29 C. Y. Khripin, X. Tu, J. M. Heddleston, C. Silvera-Batista, A. R. Hight Walker, J. Fagan and M. Zheng, *Anal. Chem.*, 2013, **85**, 1382–1388.
30 J. A. Fagan, M. L. Becker, J. Chun, P. Nie, B. J. Bauer, J. R. Simpson, A. Hight-Walker and E. K. Hobbie, *Langmuir*, 2008, **24**, 13880–13889.
31 J. A. Fagan, M. L. Becker, J. Chun and E. K. Hobbie, *Adv. Mater.*, 2008, **20**, 1609–1613.
32 S. Ohmori, T. Saito, B. Shukla, M. Yumura and S. Iijima, *ACS Nano*, 2010, **4**, 3606–3610.
33 J. Chun, J. A. Fagan, E. K. Hobbie and B. J. Bauer, *Anal. Chem.*, 2008, **80**, 2514–2523.
34 C. Y. Khripin, N. Arnold-Medabalimi and M. Zheng, *ACS Nano*, 2011, **5**, 8258–8266.
35 H. Chen, Y. Cao, J. Zhang and C. Zhou, *Nat. Commun.*, 2014, **5**, 4097.
36 J. Zhang, H. Gui, B. Liu, J. Liu and C. Zhou, *Nano Res.*, 2013, **6**, 906–920.
37 F. S. Bates, *Science*, 1991, **251**, 898–905.
38 C. Wang, J. Zhang, K. Ryu, A. Badmaev, L. G. De Arco and C. Zhou, *Nano Lett.*, 2009, **9**, 4285–4291.
39 N. Rouhi, D. Jain and P. J. Burke, *ACS Nano*, 2011, **5**, 8471–8487.
40 G. J. Brady, Y. Joo, M. Y. Wu, M. J. Shea, P. Gopalan and M. S. Arnold, *ACS Nano*, 2014, 11614–11621.